

Hybrid kernel polynomial method

Muhammad Irfan,¹ Sathish R. Kuppuswamy,¹ Dániel Varjas,^{2,1,*} Pablo M. Perez-Piskunow,^{1,3} Rafal Skolasinski,^{2,1} Michael Wimmer,^{2,1} and Anton R. Akhmerov¹

¹*Kavli Institute of Nanoscience, Delft University of Technology,
P.O. Box 4056, 2600 GA Delft, The Netherlands*

²*QuTech, Delft University of Technology, P.O. Box 4056, 2600 GA Delft, The Netherlands*

³*Catalan Institute of Nanoscience and Nanotechnology (ICN2),
CSIC and BIST, Campus UAB, Bellaterra, 08193 Barcelona, Spain*

The kernel polynomial method allows to sample overall spectral properties of a quantum system, while sparse diagonalization provides accurate information about a few important states. We present a method combining these two approaches without loss of performance or accuracy. We apply this hybrid kernel polynomial method to improve the computation of thermodynamic quantities and the construction of perturbative effective models, in a regime where neither of the methods is sufficient on its own. We demonstrate the efficiency of our approach on three examples: the calculation of supercurrent and inductance in a Josephson junction, the interaction of spin qubits defined in a two dimensional electron gas, and the calculation of the effective band structure in a realistic model of a semiconductor nanowire.

I. INTRODUCTION

The behavior of the Fermi sea is governed by both the few partially occupied states near the Fermi level, and the overall effect of the large number of fully occupied states. Therefore, in order to accurately capture the relevant physics, one needs to combine high resolution information about the former with integrated contribution of the latter. A similar need to combine integrated information with high resolution arises when constructing effective models using Löwdin partitioning or Schrieffer-Wolff transformation [1–4]. In a computational context, simultaneously satisfying these two requirements is only possible with the full knowledge of the spectrum. Therefore analyzing a system with size N Hilbert space requires the full cost of $\mathcal{O}(N^3)$ operations of dense linear algebra, prohibiting the exploitation of the sparsity of the Hamiltonian.

Applying a sparse Hamiltonian to a state is cheap. Iterative diagonalization algorithms efficiently utilize this to obtain a small set of eigenenergies and eigenvectors at a low cost [5]. For example, the algorithms implemented in ARPACK [6] combined with a sparse direct linear solver (such as MUMPS [7, 8]) allow to compute several eigenvectors around any interior point of the spectrum. The kernel polynomial method (KPM) [9] also utilizes the sparsity structure, but to obtain limited energy resolution information about the full spectrum. This is possible due to recursive computation of the Chebyshev decomposition of the Hamiltonian action on a vector.

In this work we propose a family of algorithms which we call “hybrid KPM” that combine the integral information of KPM with the high precision of diagonalization. The building block of these methods is the amended KPM expansion, where we subtract the contribution of the known part of the spectrum. Hybrid KPM algorithms apply

both to the computation of thermodynamic properties at low temperatures, and the construction of effective Hamiltonians restricted to a small subspace. We demonstrate on a set of physical problems that hybrid KPM achieves increased precision at the same computational cost.

We apply and benchmark hybrid KPM by computing supercurrent and Josephson inductance of a long Josephson junction [10–12], where both the contribution of discrete subgap states and the continuum are of the same order. Turning to the effective models, we consider two model systems: tunneling Hamiltonian of two coupled quantum dots [13], and band structure of a semiconductor nanowire [14–17]. In both cases we start from a microscopic Hamiltonian and obtain an accurate effective model, which requires using up to 4th order perturbation theory.

II. KERNEL POLYNOMIAL METHOD

To compute thermodynamic properties and effective models, one needs to evaluate the action of the Fermi function or Green’s function of the Hamiltonian on a state. The kernel polynomial method (KPM) [9] enables an efficient approximation of such functions of operators. We start by rescaling a Hamiltonian \hat{H} such that its spectrum $\{E_k\}$ is bounded to the interval $(-1, 1)$. In general, a function $f(\hat{H}, \lambda)$ of a Hermitian operator \hat{H} and a set of parameters λ can be calculated using the eigendecomposition $\hat{H} = \sum_k E_k |\psi_k\rangle\langle\psi_k|$ as

$$f(\hat{H}, \lambda) \equiv \sum_k f(E_k, \lambda) |\psi_k\rangle\langle\psi_k|, \quad (1)$$

where $f(E, \lambda)$ is a scalar function. The expansion in eigenfunctions is computationally expensive since it requires the full diagonalization of \hat{H} . This process scales as $\mathcal{O}(N^3)$ with the N size of the Hilbert space.

an alternative approach—KPM—utilizes the expansion of the scalar function $f(E, \lambda)$ in terms of Chebyshev

* Electronic address: dvarjas@gmail.com

polynomials T_m

$$f(E, \lambda) = \sum_{m=0}^{\infty} \alpha_m(\lambda) T_m(E), \quad (2)$$

to build the operator function $f(\hat{H}, \lambda)$. The Chebyshev polynomials $T_m(x) = \cos(m \arccos x)$ form a complete basis in the interval $(-1, 1)$. They are orthogonal under the inner product

$$\langle f \cdot g \rangle = \int_{-1}^1 \frac{f(x)g(x)}{\pi \sqrt{1-x^2}} dx, \quad (3)$$

and satisfy the recursion relation $T_{m+1}(x) = 2xT_m(x) - T_{m-1}(x)$. The Chebyshev coefficients α_m are calculated using the inner product from Eq. (3) with variable E

$$\alpha_m(\lambda) = \langle f(E, \lambda) \cdot T_m(E) \rangle, \quad (4)$$

and the same coefficients apply to the polynomial expansion of the operator function

$$f(\hat{H}, \lambda) = \sum_{m=0}^{\infty} \alpha_m(\lambda) T_m(\hat{H}). \quad (5)$$

We are interested in the action of $f(\hat{H}, \lambda)$ on a set of vectors. In such situations, the expensive part of the computation is to calculate $T_m(\hat{H})|v\rangle$, and once we have done that, the coefficients can be readily computed (in most cases analytically) for any value of the parameters λ .

In practice, the magnitude of the coefficients α_m decays with m and we truncate the series to a finite order M . To stabilize the convergence and avoid Gibbs oscillations, while ensuring positivity, we use either the Jackson or Lorentz kernel [9], which introduce a set of prefactors $g_{m,M}$ that modify the coefficients to $\tilde{\alpha}_m(\lambda) = g_{m,M} \alpha_m(\lambda)$.

The error of the KPM approximation comes from the function f being replaced by its finite order Chebyshev polynomial approximation:

$$f(\hat{H}, \lambda) \stackrel{\text{KPM}}{\approx} \tilde{f}(\hat{H}, \lambda) \equiv \sum_k \tilde{f}(E_k, \lambda) |\psi_k\rangle \langle \psi_k|, \quad (6)$$

with

$$\tilde{f}(E, \lambda) = \sum_{m=0}^M \tilde{\alpha}_m(\lambda) T_m(E). \quad (7)$$

This error is small if the function is smooth, or there are no eigenvalues of \hat{H} in regions where it changes fast. The order of the approximation M , together with the choice of the kernel, sets the energy resolution of the approximation, which for the Jackson kernel is inversely proportional to M . The Chebyshev expansion of order M captures features larger than W/M , where W is the full bandwidth of \hat{H} [9].

Hamiltonians and other observables that appear in physical problems are typically sparse matrices where the number of nonzero entries is proportional to the system size N . This allows calculating a sparse matrix–vector product in $\mathcal{O}(N)$ time, much faster than the $\mathcal{O}(N^2)$ scaling of dense matrix–vector products. The recursion relation for Chebyshev polynomials can then be rewritten for the operator function acting on a vector as

$$|v_{m+1}\rangle = 2\hat{H}|v_m\rangle - |v_{m-1}\rangle, \quad (8)$$

where $|v_m\rangle = T_m(\hat{H})|v\rangle$. Hence, the Chebyshev expanded action $f(\hat{H}, \lambda)|v\rangle$ up to order M can be computed in $\mathcal{O}(NM)$ time. The computational effort of KPM scales as $\mathcal{O}(NW/\Delta)$ where Δ is the required energy resolution. KPM is most efficient when the desired energy resolution is much coarser than the typical level spacing, that is when $\Delta \gg W/N$, and $M = W/\Delta \ll N$.

As we saw above, KPM performs poorly if there are eigenstates in energy ranges where f changes rapidly, necessitating a fine energy resolution. If there are only few such states, however, we can use a sparse eigensolver to find these states and take their contribution into account exactly, while keeping the energy resolution of KPM low. This is the key idea behind hybrid KPM: we get a more accurate approximation by subtracting the KPM contribution of these states and adding back their exact contribution:

$$f(\hat{H}, \lambda) \stackrel{\text{hybrid}}{\approx} \tilde{f}(\hat{H}, \lambda) - \sum_{k \in A} \tilde{f}(E_k, \lambda) |\psi_k\rangle \langle \psi_k| + \sum_{k \in A} f(E_k, \lambda) |\psi_k\rangle \langle \psi_k|, \quad (9)$$

where A is the subspace of exactly known states.

III. LÖWDIN PERTURBATION THEORY

A. Löwdin partitioning

Physical systems often have many degrees of freedom, of which only a few (for example the lowest energy ones) are of interest for physical understanding. Such a situation can be addressed using perturbative effective models, which are restricted to the small “interesting” subspace, and integrate out the other “uninteresting” states. The effective model includes, beyond the shift in the energy of the eigenstates, terms mixing various eigenstates, providing a deeper understanding.

We use the Löwdin partitioning approach [1, 3, 4] (also known as Schrieffer–Wolff transformation [2]) to calculate the effective Hamiltonian. Conventionally, this approach requires full diagonalization of the unperturbed Hamiltonian, making it unfeasible in large systems. We find, however, that we only need to exactly know the states in the interesting subspace, while the rest can be efficiently taken into account using KPM. This allows us to

apply this method to systems with millions of degrees of freedom, as long as the interesting subspace is small.

We start by separating initial Hamiltonian into unperturbed part H_0 and perturbation with λ_α as small parameters:

$$H = H_0 + \sum_{\alpha} \lambda_{\alpha} H'_{\alpha}. \quad (10)$$

Assuming that the eigenstates and energies of H_0 are known

$$H_0 |\psi_n\rangle = E_n |\psi_n\rangle, \quad (11)$$

we split states $|\psi_n\rangle$ into two groups, A and B . We are interested in states from group A whereas effect of states B we want to include via perturbation theory. We assume that these two groups of states are separated in energy, but states within A and B may be degenerate. The goal is to find a unitary basis transformation with skew-Hermitian S as

$$\tilde{H} = e^{-S} H e^S, \quad (12)$$

such that the transformed Hamiltonian \tilde{H} does not couple the A and B subspaces, and the block in the A subspace is the effective Hamiltonian, $H_{\text{eff}} = \tilde{H}_{AA}$. We find S and H_{eff} order-by-order in the small parameters (for details see Appendix B):

$$H_{\text{eff}} = \tilde{H}^{(0)} + \sum_{\alpha} \lambda_{\alpha} \tilde{H}^{(1,\alpha)} + \sum_{\alpha\beta} \lambda_{\alpha} \lambda_{\beta} \tilde{H}^{(2,\alpha\beta)} + \dots \quad (13)$$

When the A subspace corresponds to a single eigenvalue, that is possibly degenerate, the Löwdin perturbation theory reproduces the conventional perturbation theory.

B. The KPM approximation of effective Hamiltonian

To provide a concrete example, we consider the second order effective Hamiltonian with one small parameter,

$$H_{\text{eff}} = \tilde{H}^{(0)} + \lambda \tilde{H}^{(1)} + \lambda^2 \tilde{H}^{(2)}, \quad (14a)$$

with the explicit terms

$$\tilde{H}_{mn}^{(0)} = E_m \delta_{m,n}, \quad (14b)$$

$$\tilde{H}_{mn}^{(1)} = \langle \psi_m | H' | \psi_n \rangle, \quad (14c)$$

$$\begin{aligned} \tilde{H}_{mn}^{(2)} = \frac{1}{2} \sum_{l \in B} & \left(\frac{\langle \psi_m | H' | \psi_l \rangle \langle \psi_l | H' | \psi_n \rangle}{E_m - E_l} \right. \\ & \left. + \frac{\langle \psi_m | H' | \psi_l \rangle \langle \psi_l | H' | \psi_n \rangle}{E_n - E_l} \right), \quad (14d) \end{aligned}$$

where m and n index states of the A subspace and l indexes states of the B subspace.

We rewrite the first term in the second order contribution as

$$\begin{aligned} \sum_{l \in B} \frac{\langle \psi_m | H' | \psi_l \rangle \langle \psi_l | H' | \psi_n \rangle}{E_m - E_l} &= \\ &= \langle \psi_m | H' \left(\sum_{l \in B} \frac{|\psi_l\rangle \langle \psi_l|}{E_m - E_l} \right) H' | \psi_n \rangle = \\ &= \langle \psi_m | H' P_B G_0(E_m) P_B H' | \psi_n \rangle, \quad (15) \end{aligned}$$

where G_0 is the unperturbed Green's function

$$G_0(E) = \frac{1}{E - H_0} = \sum_i \frac{|\psi_i\rangle \langle \psi_i|}{E - E_i}, \quad (16)$$

and P_B is the projector onto the B subspace.

This formulation is well suited for approximate evaluation using the KPM expanded Green's function. The Green's function only acts on a small set of vectors, $|\phi_n\rangle = P_B H' |\psi_n\rangle$ for $n \in A$. The exact eigenstates of the A subspace can be obtained using sparse diagonalization of H_0 , while it is not necessary to know the B eigenvectors using $P_B = \mathbb{1} - P_A$. These states $|\phi_n\rangle$ are purely in the B subspace, with the energy argument of G_0 in the A subspace. The energy gap between the two sets of states ensures that all divergences are avoided, and the action of G_0 can be approximated using KPM. After these substitutions, the second order contribution simplifies to

$$\tilde{H}_{mn}^{(2)} = \frac{1}{2} \langle \phi_m | G_0(E_m) | \phi_n \rangle + \frac{1}{2} \langle \phi_m | G_0(E_n) | \phi_n \rangle. \quad (17)$$

Similar simplification in terms of G_0 is also possible for all higher orders, for details see Appendix C.

C. Effective Hamiltonian with hybrid KPM

In order to accurately approximate the action of G_0 on B states closest to the A subspace in energy, we need to choose the number of Chebyshev moments at the order of W/Δ , where W is the full bandwidth of H_0 and Δ is the gap between A and B states. Hence, for small Δ accurate calculation using KPM becomes computationally expensive. Alternatively, knowing all the B eigenstates would allow exact evaluation of the Green's function, at even higher computational cost.

To solve this problem, we propose the hybrid KPM approach, where only a subset B_e of the B eigenstates is known explicitly. These we choose to be the eigenstates with closest energy to the A states, and are obtained using sparse diagonalization. We split the Green's function of the B subspace to two terms:

$$G_0(E) P_B = \sum_{l \in B_e} \frac{|\psi_l\rangle \langle \psi_l|}{E - E_l} + G_0^{\text{KPM}}(E) (P_B - P_{B_e}), \quad (18)$$

where P_B and P_{B_e} are projectors to the B and B_e subspaces, and G_0^{KPM} is the KPM approximated Green's function.

IV. COMPUTATION OF THERMODYNAMIC QUANTITIES

A. Evaluation of operator expectation values

Physical observables in a non-interacting fermionic system are often expressed as the expectation value of a Hermitian operator \hat{A} as

$$\langle \hat{A} \rangle_{E_F} = \sum_k f(E_k, E_F) \langle \psi_k | \hat{A} | \psi_k \rangle, \quad (19)$$

where the sum runs over all eigenstates of the Hamiltonian $|\psi_k\rangle$ with eigenenergies E_k . The occupation of the states is given by the Fermi function

$$f(E, E_F) = \frac{1}{e^{\beta(E-E_F)} + 1} \quad (20)$$

with $\beta = (k_B T)^{-1}$ and E_F the Fermi energy. This can be rewritten as a trace using the operator function formalism introduced above, which can be readily evaluated using KPM:

$$\langle \hat{A} \rangle_{E_F} = \text{Tr} \left[\hat{A} f(\hat{H}, E_F) \right] = \sum_m \tilde{\alpha}_m(E_F) \mu_m, \quad (21)$$

where full KPM the moments are

$$\mu_m = \text{Tr} \left[\hat{A} T_m(\hat{H}) \right]. \quad (22)$$

Inserting a delta function, we can also express this quantity as an integral over the spectral density of the operator $A(E) = \text{Tr} \left[\hat{A} \delta(E - \hat{H}) \right]$:

$$\langle \hat{A} \rangle_{E_F} = \int dE f(E, E_F) A(E). \quad (23)$$

The Chebyshev expansion has a finite energy resolution of W/M (where W is the bandwidth of the spectrum), and might not be enough to resolve sensitive features near the Fermi level. In this case, we apply a hybrid approach, where states near the Fermi level are solved very accurately with a sparse eigenvalue solver, while the rest of the spectrum is treated using KPM.

When evaluating the KPM moments of the operator, we split the trace into two parts: states that belong to the exactly known subspace A and states that belong to the rest of the Hilbert space B :

$$\begin{aligned} \mu_m &= \mu_m^A + \mu_m^B = \\ &= \sum_{i \in A} \langle \psi_i | \hat{A} T_m(\hat{H}) | \psi_i \rangle + \sum_{j \in B} \langle \psi_j | \hat{A} T_m(\hat{H}) | \psi_j \rangle. \end{aligned} \quad (24)$$

Using the moments μ^B eliminates the contributions from states near the Fermi level, which we add back using the

exact eigenstates $|\psi_i\rangle$ obtained from sparse diagonalization:

$$\langle \hat{A} \rangle_{E_F} = \sum_m \tilde{\alpha}_m(E_F) \mu_m^B + \sum_{i \in A} f(E_i, E_F) \langle \psi_i | \hat{A} | \psi_i \rangle. \quad (25)$$

We evaluate the contribution of the B subspace without knowing the complete set of B eigenvectors, by subtracting the A subspace KPM contribution from the full KPM result, $\mu_m^B = \mu_m - \mu_m^A$. The trace in the full contribution is efficiently approximated using the stochastic trace approximation [9]. The exact evaluation of the trace is also feasible if the operator \hat{A} has low rank and the basis of its image space is explicitly known:

$$\mu_m = \sum_{|\psi\rangle \in \text{Im } \hat{A}} \langle \psi | \hat{A} T_m(\hat{H}) | \psi \rangle. \quad (26)$$

This hybrid method provides an accurate treatment of the contribution of a few states near the Fermi level, while the contribution from the rest of the spectrum is efficiently evaluated using KPM with a small number of moments.

B. Perturbation expansion of expectation values

As we saw, KPM offers efficient evaluation of traces, here we generalize the KPM expansion to allow order-by-order expansion of such quantities in small perturbations to the Hamiltonian. We consider a generic function g and perturbed Hamiltonian $\hat{H} = \hat{H}_0 + \lambda \hat{H}_1$ where λ is a small parameter. We want to evaluate $\text{Tr} \left[g(\hat{H}) \right]$ order by order in the small parameter. For example, we can write the expectation value of the energy of the filled Fermi sea as $\langle E \rangle = \text{Tr} \left[g(\hat{H}) \right]$ with $g(E) = Ef(E)$ where f is the Fermi function. The argument below also applies to expressions of the form $\text{Tr} \left[\hat{A} g(\hat{H}) \right]$, but we restrict to the $\hat{A} = \mathbb{1}$ case for brevity.

The key insight is that KPM is well suited for the evaluation of such perturbative series with one minor modification: we allow \hat{H} to depend on small parameters. The recursion relation (8) for the KPM-expanded vectors remains valid if we allow \hat{H} and $|v_m\rangle$ to be polynomials of λ . If we are only interested in the result up to λ^n order, we can discard all higher order terms at every step of the iteration, resulting in KPM moments μ_m and an overall result that is also an n 'th order polynomial of λ . This method produces the exact series expansion of the result if the function g can be represented exactly by its Chebyshev polynomial expansion. The resulting increase in computational cost scales as $\mathcal{O}(n^2)$, making this method feasible at low orders.

A rearrangement of the terms in the perturbation expansion allows us to efficiently calculate the trace when the image space of the perturbation H_1 is small. Using

cyclic permutation of terms inside the trace, the first order correction (which is the same as the λ -linear term in the expansion) can be written as

$$\frac{d}{d\lambda} \text{Tr} \left[g(\hat{H}) \right]_{\lambda=0} = \text{Tr} \left[g'(\hat{H}_0) \hat{H}_1 \right] \quad (27)$$

where g' is the derivative of g . As \hat{H}_1 is always on the right, the trace can be replaced by a sum over a basis of the image space of \hat{H}_1 . Applying this to the energy expectation value in the zero temperature limit where f is a step function (using that $x\delta(x) = 0$) we get

$$\begin{aligned} \frac{d}{d\lambda} \langle E \rangle_{\lambda=0} &= \frac{d}{d\lambda} \text{Tr} \left[\hat{H} f(\hat{H}) \right]_{\lambda=0} = \\ &= \text{Tr} \left[f(\hat{H}_0) \hat{H}_1 \right] = \langle \hat{H}_1 \rangle_{\lambda=0} \end{aligned} \quad (28)$$

which is the same as the ground state expectation value of H_1 , and was already discussed in the previous section. Similar rearrangement is also possible at all higher orders, here we present the second order case in detail. For a generic function g and Hamiltonian $\hat{H} = \hat{H}_0 + \lambda \hat{H}_1 + \lambda^2 \hat{H}_2$, by expanding and rearranging terms containing λ^2 we find

$$\begin{aligned} \frac{1}{2} \frac{d^2}{d\lambda^2} \text{Tr} \left[g(\hat{H}) \right]_{\lambda=0} &= \\ = \text{Tr} \left[g'(\hat{H}_0) \hat{H}_2 \right] + \frac{1}{2} \frac{d}{d\lambda} \text{Tr} \left[g'(\hat{H}) \hat{H}_1 \right]_{\lambda=0} \end{aligned} \quad (29)$$

We can use the basis of the image spaces of \hat{H}_2 and \hat{H}_1 respectively in the two terms. To obtain the second term we use the KPM expansion to first order in λ .

The above method is only accurate if the function g and its derivatives can be accurately represented by its Chebyshev polynomial expansion. If there are eigenvalues of the Hamiltonian in the range where g changes rapidly (for example near the Fermi level), the number of moments required for an accurate approximation makes the calculation prohibitively expensive. Using perturbation theory on a few, exactly known low lying states (A subspace) allows us to extend the hybrid approach to higher order perturbative expansions. As already mentioned, the error in KPM results from the function g being replaced by its Chebyshev approximation \tilde{g} :

$$\text{Tr} \left[g(\hat{H}) \right] \stackrel{\text{KPM}}{\approx} \text{Tr} \left[\tilde{g}(\hat{H}) \right] = \sum_k \tilde{g}(E_k). \quad (30)$$

With the energies E_k of the A subspace states available as a power series, we get a more accurate approximation by subtracting the KPM contribution of these states and adding back the exact contribution:

$$\text{Tr} \left[g(\hat{H}) \right] \stackrel{\text{hybrid}}{\approx} \text{Tr} \left[\tilde{g}(\hat{H}) \right] - \sum_{k \in A} \tilde{g}(E_k) + \sum_{k \in A} g(E_k). \quad (31)$$

With the exact derivatives of g and \tilde{g} known, we obtain the final result as a power series.

We utilize the hybrid KPM Löwdin perturbation theory developed in Sec. III to get the perturbation series of the A subspace eigenenergies. We treat a single eigenpair $(E_k, |\psi_k\rangle)$ of \hat{H}_0 as the A subspace for the purposes of Löwdin perturbation theory, and use the rest of the exactly known states as the B_e subspace in the hybrid evaluation of the Green's function. Repeating this for every A eigenstate produces the set of power series expansions for the perturbed E_k up to the desired order. This method produces the most accurate perturbative expansion for states in the middle of the A subspace energy range, this is chosen to coincide with the fastest-changing region of g' . For states close to the edge of the energy range the perturbative expansion is less accurate, but, at the same time, the difference between g and \tilde{g} is also small, resulting in a small overall error.

This analysis leaves some questions open: What are the convergence properties of the stochastic trace evaluation of the KPM perturbation series for generic perturbation Hamiltonians? What is the general form of rearranged equations similar to (29) for higher orders and multiple perturbation parameters? What is the optimal way to choose the A and B_e subspaces and the number of KPM moments for the Löwdin perturbation theory? How does the efficiency of our method compare to other recursive numerical approaches to perturbation theory, such as Ref. 18? These we leave to future work.

V. APPLICATIONS

A. Supercurrent and Josephson inductance

We apply the hybrid KPM method to calculate supercurrent in a Josephson junction [10]. Josephson junctions have two distinct limits [11, 12]: the short-junction regime where Thouless energy E_T is much larger than the superconducting gap Δ and the long-junction regime with $E_T \ll \Delta$. In the short junction regime, because the energies of states above the gap do not depend on the superconducting phase difference, the supercurrent is solely carried by Andreev bound states. As a result, the calculation of supercurrent is computationally less expensive because we only need the eigenvalues within the superconducting gap. However, in a long Josephson junction, the continuum states also vary as a function of the superconducting phase difference and contribute to the total supercurrent [19]. Therefore, the calculation of supercurrent involves the entire spectrum, which is computationally expensive. In the hybrid KPM approach we calculate the subgap states using exact diagonalization, and estimate the contribution of continuum states using KPM.

We consider a Josephson junction of normal region length L_N , superconducting leads of length L_S and width W as shown in the inset of Fig. 1. For simplicity, we consider a spinless Bogoliubov-de Gennes (BdG) Hamiltonian

without magnetic field:

$$H_{BdG} = \begin{pmatrix} \frac{\mathbf{p}^2}{2m} - \mu & \Delta(x) \\ \Delta^*(x) & \mu - \frac{\mathbf{p}^2}{2m} \end{pmatrix}, \quad (32)$$

with \mathbf{p} the momentum operator, m the effective electron mass, and μ the chemical potential. The superconducting order parameter $\Delta(x)$ is zero in the normal region whereas has value $\Delta \exp(i\phi_L)$ in the left and $\Delta \exp(i\phi_R)$ in the right superconducting lead. If we connect the left and right superconductors in a SQUID geometry, the phase difference $\phi = \phi_R - \phi_L$ measures the magnetic flux through the loop in $\hbar/(2e)$ units. We discretize this Hamiltonian on a square lattice of mesh size a with a tight-binding hopping parameter $t = \hbar^2/(2ma^2)$. To calculate supercurrent, we define a current operator \hat{I} across a cut in the normal scattering region parallel to the normal-metal – superconductor interface (see the inset of Fig. 1), the block connecting sites i and j is given by:

$$\hat{I}_{ij} = \frac{e}{\hbar} \times \begin{cases} iH_{ij}\tau_z & \text{if } i \in L \text{ and } j \in R \\ -i\tau_z H_{ij} & \text{if } i \in R \text{ and } j \in L \\ 0 & \text{otherwise} \end{cases} \quad (33)$$

with H_{ij} the hopping Hamiltonian between site i and j in the BdG formalism, τ_z the Pauli matrix in particle-hole space and L/R corresponding to the left and right side of the cut. As the current operator is only supported on the sites next to the cut, when calculating the trace

$$\langle \hat{I} \rangle = \text{Tr} \left[\hat{I} f(\hat{H}) \right] \quad (34)$$

for the KPM contribution, we use a full basis of these states. All other states are annihilated by the current operator and do not contribute to the current.

We consider a Josephson junction of length $L_N = L_S = 50a$ and width $W = 15a$ and set the parameters $\mu = 0.2t$ and $\Delta = 0.15t$. As explained in sec. IV, we calculate the subgap Andreev bound states exactly using sparse diagonalization and treat them as the A subspace. We show the spectral density of the current operator $I(E)$ in Fig. 1, where we illustrate the contributions of subgap and continuum states separately. The solid blue line is the KPM only spectrum of the current operator, which vanishes at this resolution with $M = 500$ moments. In the hybrid approach, the exactly known subgap states contribute Dirac delta peaks, whereas the contribution of only the continuum states calculated with KPM is non-vanishing.

In Fig. 2, we show the current-phase relation with contribution from the Andreev states (solid blue curve) as well as the continuum states (black curve). The orange curve shows the total supercurrent. It is evident that the contributions of both the subgap and the continuum states are significant, as shown by the gray filled area under the total supercurrent.

In order to calculate the Josephson inductance of the junction, first we derive the expression for the supercurrent (34) from a different starting point. We apply a

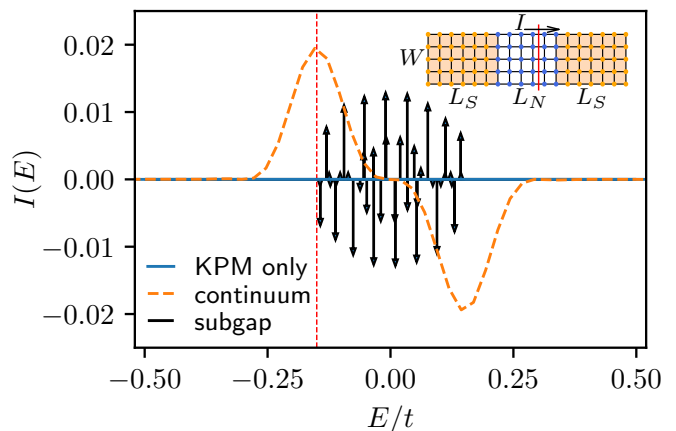


FIG. 1. Current operator spectrum as a function of energy with fixed relative superconducting phase of $\pi/2$. The solid blue line represents the KPM only spectrum of the current operator; the arrows represent the Dirac delta contributions of subgap states; the dashed orange line shows the contribution of the continuum states. Inset: Sketch of the system (not the actual size used in the numerics). The shaded regions are superconducting with a normal region in the middle. The red line represents the cut for which we calculate the supercurrent.

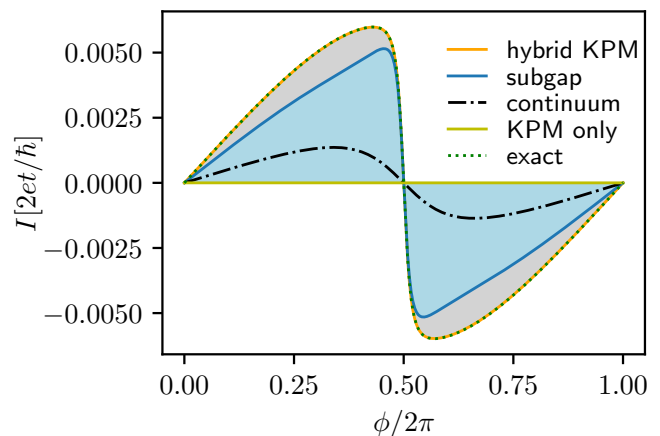


FIG. 2. Supercurrent as a function of the superconducting phase difference. The orange line represents the total supercurrent through a Josephson junction calculated with hybrid KPM, whereas the blue and black lines show the corresponding contributions from subgap and continuum states respectively. The hybrid KPM result agrees with the exact result using full diagonalization, while the KPM only result vanishes using the same number of moments.

gauge transformation $U(i) = \exp(i\phi(i)\tau_z/2)$ that acts differently on the left and right side of the cut (see Fig. 1 inset). Choosing $\phi(i) = -\phi_L$ if $i \in L$ and $\phi(i) = -\phi_R$ if $i \in R$, we can ensure that the superconducting phase is zero in both the left and right leads. This gauge concentrates all the phase change on the bonds crossing the cut,

with modified hoppings

$$H_{ij} \rightarrow \begin{cases} H_{ij} \exp(i\phi\tau_z/2) & \text{if } i \in L \text{ and } j \in R \\ \exp(-i\phi\tau_z/2)H_{ij} & \text{if } i \in R \text{ and } j \in L \\ H_{ij} & \text{otherwise} \end{cases} \quad (35)$$

where we chose $\phi_L = 0$ without loss of generality. The current operator across the cut is given by the derivative of the Hamiltonian with respect to the flux:

$$\hat{I} = \frac{2e}{\hbar} \frac{d\hat{H}}{d\phi}, \quad (36)$$

which reproduces (34).

The inverse of the inductance of the junction can be calculated as the derivative of the current expectation value with respect to the flux:

$$L_J^{-1} = \frac{(2e)^2}{\hbar^2} \frac{d^2}{d\phi^2} \langle \hat{H} \rangle. \quad (37)$$

We evaluate this expression using the hybrid method discussed in Sec. IV B taking into account the second derivative of the Hamiltonian, the result is shown in Fig. 3. The sharp peak in L_J^{-1} at $\phi = \pi$ is accurately captured by the direct evaluation of the second derivative using our method, while accurate calculation using a discrete derivative of the current expectation value requires a much higher resolution in ϕ . The figure also illustrates that the separation to continuum and subgap contributions for the inductance is not the same as for the current, but the total results agree.

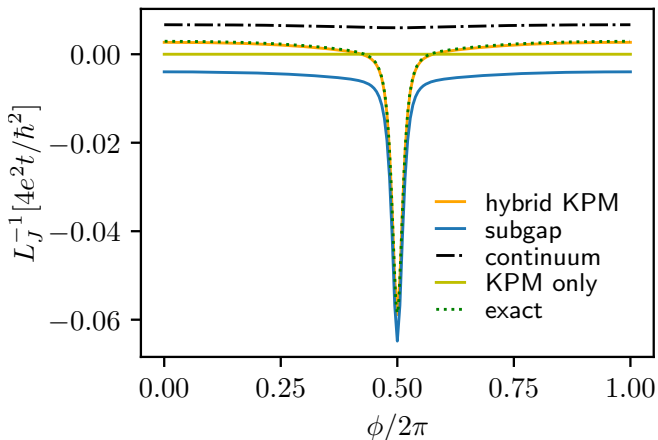


FIG. 3. Inverse Josephson inductance as a function of the superconducting phase difference. The orange line represents L_J^{-1} calculated with hybrid KPM, whereas the blue and black lines show the corresponding contributions from subgap and continuum states respectively. The hybrid KPM result agrees with the exact result using full diagonalization, while the KPM only result vanishes using the same number of moments.

In this section we only considered the zero temperature limit. We emphasize, however, that including finite temperature is straightforward, merely requires replacing f

with the Fermi function at the correct temperature. In fact, a temperature sweep is essentially free using our method, as computation of the KPM moments and the perturbation expansion of low lying states is the costliest part numerically. The exact form of f only enters in the last step, and all previous data can be reused.

B. Effective Hamiltonian of spin qubits

We apply hybrid KPM to calculate an effective Hamiltonian for the lowest few energy states in a spin qubit system. As an example, we consider two gate defined quantum dots with the interdot tunnel coupling and dot chemical potential controlled by the gate electrodes. To study the device characteristics under different bias conditions, we consider a simple effective model including an in-plane gate confinement term. We discretize the effective model to obtain a tight-binding Hamiltonian and finally diagonalize it to obtain the energy spectrum. Since gate voltages are adjusted in these systems to produce well-defined qubits in a scalable way, we consider small changes in gate voltage as perturbation. In order to derive an effective Hamiltonian in the basis of individual quantum dot states, we start with a system with decoupled dots and include hoppings between the dots perturbatively. The eigenfunctions and eigenenergies of the lowest few bound states in the quantum dots are included exactly in the effective model whereas we treat the remaining part of the energy spectrum up to third order in the Löwdin perturbation theory using hybrid KPM approach.

We form two quantum dots by depleting the two dimensional electron gas (2DEG) confined in the GaAs/AlGaAs heterostructure [13]. In our simulations, we place the gate electrodes at 60nm above the 2DEG in growth direction and pattern them according to the gate design from Ref. 13. A positive global back gate is used to accumulate carriers in the 2DEG whereas applying negative voltage to the top gate electrodes depletes the 2DEG forming two quantum dots. *Plunger* gates control the dot chemical potential whereas the tunnel barrier height between dots is controlled by the *barrier* gates shown in between two plunger gates in Fig. 4. We follow the approach from [20] to calculate the electrostatic potential induced in the 2DEG due to the gate electrodes. We determine the voltages of different gate electrodes required to form two tunnel coupled quantum dots and plotted the corresponding 2D electrostatic potential in Fig. 4.

To describe the 2DEG, we use a two dimensional continuum Hamiltonian

$$H_{2D} = \frac{\hbar^2}{2m_e} (\mathbf{k}_x^2 + \mathbf{k}_y^2) + V(x, y), \quad (38)$$

where m_e is the effective electron mass in GaAs, k_x and k_y are the particle momentum and $V(x, y)$ is the 2D gate-induced confinement potential. We discretize the continuum Hamiltonian H_{2D} using finite difference scheme included in the Kwant software package [21]. We choose

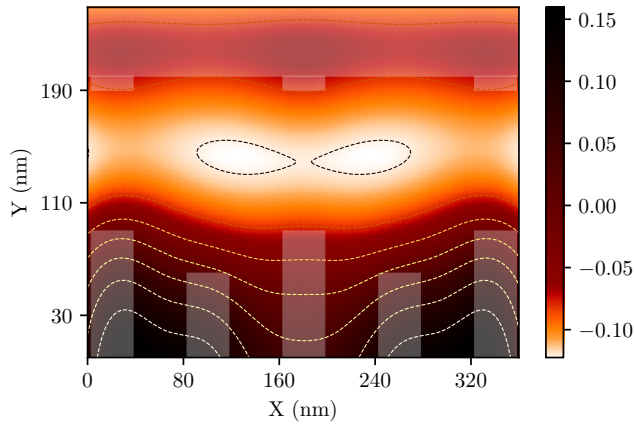


FIG. 4. The 2DEG electrostatic potential superimposed with gate electrodes deposited on top of the GaAs heterostructure. We use the gate design and heterostructure from [13]. Plunger and barrier gates are shown at the bottom and screening gates at the top. By applying negative voltage to the gate electrodes, we locally deplete the 2DEG to form two quantum dots as represented by the equipotential lines.

5nm lattice spacing and nearest neighbour hopping to obtain a tight binding model on the square lattice with onsite and hopping terms. We use this tight binding Hamiltonian in the following.

We define the Hamiltonian as a sum of unperturbed H_0 term and two perturbation terms as follows

$$H = H_0 + \lambda_g H_{gate} + \lambda_c H_{coup}, \quad (39)$$

where H_{gate} is the gate potential, H_{coup} includes hoppings between the right and left dot, while these hoppings are removed from H_0 . λ_g and λ_c control the strengths of perturbation in the effective model. We split the spectrum of the Hamiltonian into two subspaces: A contains few lowest bound states in the quantum dots for which we determine the effective Hamiltonian, and B represents the remaining part of the energy spectrum. The states in A and a few states $B_e \subset B$ closest to A are obtained from sparse diagonalization. We set $\lambda_c = 1$ to reproduce the 2DEG Hamiltonian without the cut between the dots. We change the chemical potential of right and left dot in opposite direction by detuning the respective gates. Considering a finite λ_c makes the off-diagonal elements in the effective Hamiltonian large enough to lift the degeneracy whereas the gate detuning leads to *avoided level crossings* in the energy spectrum as shown in Fig. 5. We do not consider coulomb interactions in our calculations, but we demonstrate the efficiency of hybrid KPM to calculate effective Hamiltonian in spin qubit systems in the free electron limit, which can be used as a starting point for further study. In Fig. 5, we have compared the eigenenergies calculated from effective model having first and third order terms against the exact energies obtained from the sparse diagonalization. It is evident that the effective model with first order terms alone cannot reproduce

exact energies whereas Löwdin perturbation combined with KPM expansion up to third order shows a good agreement.

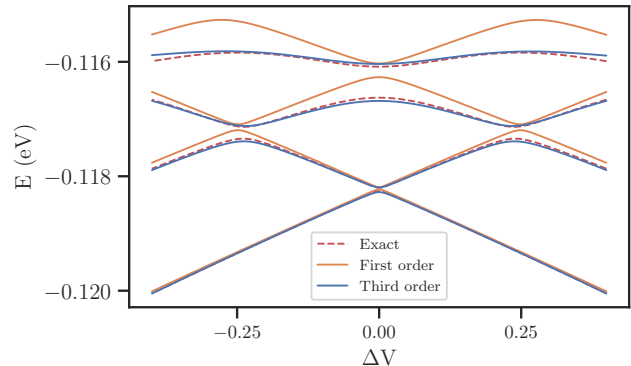


FIG. 5. Energy spectrum as a function of gate voltage difference between the two dots. Eigenenergies calculated from the first and third order effective models are compared against the exact energies.

C. Effective band structures

Semiconductor nanowires, besides many potential applications [14], are of interest as a platform to realize Majorana fermions when proximitized with a superconductor [15–17]. The key ingredients are spin-orbit interaction and external magnetic field, which remove spin degeneracy in the lowest subband of the wire, resulting in effective p -wave superconducting pairing. In an external electric field normal to the wire the bulk spin-orbit coupling of the semiconductor results in Rashba spin-orbit interaction. The interesting physics can be captured using a 2-band effective model

$$H = \frac{\hbar^2}{2m^*} k_z^2 + \mu + \alpha k_z (\sigma_y E_x + \sigma_x E_y) + \mu_B \mathbf{B} g \boldsymbol{\sigma}, \quad (40)$$

where m^* is the effective mass of the lowest subband, k_z is the momentum along the wire, μ is the chemical potential, E_x and E_y are components of the electric field, $\boldsymbol{\sigma}$ are the Pauli matrices and α characterizes the strength of the Rashba spin-orbit interaction. The external magnetic field is \mathbf{B} , μ_B is the Bohr-magneton and g is the effective g -factor tensor in the lowest subband. While this simple model is easy to solve, extracting the parameters for realistic setups is nontrivial.

We use the 8-band $\mathbf{k} \cdot \mathbf{p}$ model of bulk zinc-blende materials, in particular InAs [4, 22, 23]. This continuum model accurately captures the s conduction and p valence bands near the Fermi level at small momenta, up to second order in k . After replacing momenta k_x and k_y with spatial derivatives, we discretize this Hamiltonian using Kwant [21] in an infinite wire geometry with approximately circular cross-section in the xy plane with radius

R. We include both the Zeeman term with the bulk g -factor $g^* = -15$ of InAs [4, 24] and the orbital magnetic field using Peierls substitution [25], as well as the electrostatic potential $V = -E_x x - E_y y$. For this example we use radius $R = 5$ nm with discretization grid lattice constant $a = 0.2$ nm. This results in a tight-binding model with 31056 degrees of freedom.

We use the Löwdin algorithm treating the tight binding Hamiltonian with vanishing external fields and $k_z = 0$ as the unperturbed Hamiltonian, and include perturbations up to second order in k_z and the electric field, and up to linear order in the magnetic field. Using second order perturbation theory, we obtain the effective model of the form of (40) with $m^* = 0.036m_0$, $\alpha = 0.81$ nm², $\mu = 0.55$ eV + (20 nm²/eV) \mathbf{E}^2 , $g_{xx} = g_{yy} = -15.3$ and $g_{zz} = -15.6$, with m_0 the free electron mass and all other terms approximately vanishing. This perturbative treatment, only accurate at small parameter values, does not capture the overall energy shift of the subbands resulting from the electrostatic field at field strengths relevant to experiments. Hence, we also construct the effective model using $E_{x0} = 0.1$ eV/nm as the unperturbed Hamiltonian. The resulting spectrum at finite k_z and B_z agrees with the exact eigenenergies of the full model as illustrated in Fig. 6.

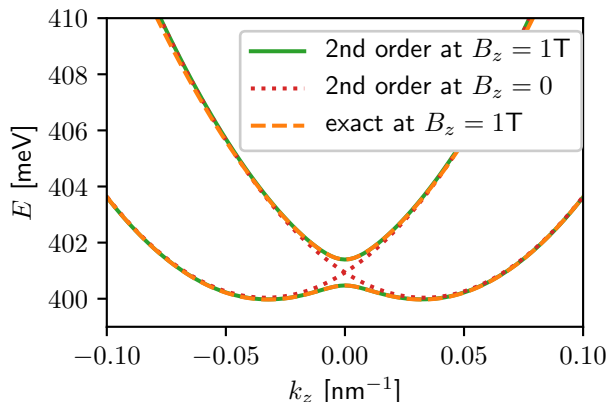


FIG. 6. Energy spectrum of the lowest subband of an InAs nanowire of radius 5 nm. The plot shows the exact result from sparse diagonalization with $B_z = 1$ T and $E_x = 0.1$ eV/nm, and the perturbation theory result around $E_{x0} = 0.1$ eV/nm at 2nd order at $B_z = 0$ and $B_z = 1$ T.

VI. CONCLUSIONS

We developed the hybrid kernel polynomial method, where we combine the strengths of KPM in treating many states at a low energy resolution and of sparse diagonalization in treating few states with high accuracy. We applied this method in multiple situations including accurate calculation of expectation values, perturbation theory

of thermodynamic quantities and construction of perturbative effective models. The source code of these general and reusable algorithms is available at [26], together with the source code and data of the examples showcased in the manuscript.

We took our examples from a variety of active research topics in condensed matter and mesoscopic physics: calculation of supercurrent and inductance in a Josephson junction, design of spin qubits defined in a two dimensional electron gas, and the calculation of the effective band structure in a realistic model of a semiconductor nanowire. Our examples illustrate how combination of low and high resolutions enables the investigation of response functions and effective models in systems whose size would make this prohibitively expensive using other approaches.

As our method allows treatment of Hilbert spaces up to millions of degrees of freedom, we expect applications beyond the non-interacting electron limit. Accurate simulation of nanoelectronic devices with truncated few-electron Hilbert spaces is a promising future direction of research using this cutting-edge methodology.

ACKNOWLEDGMENTS

We are thankful to T. Rosdahl and J. B. Weston for their role in the development of Qsymm [27], the data structures of which the implementation of our algorithms relies on. This work was supported by ERC Starting Grant 638760, the Netherlands Organisation for Scientific Research (NWO/OCW) as part of the Frontiers of Nanoscience program, NWO VIDI grant 680-47-53, the US Office of Naval Research, and the European Union's Horizon 2020 research and innovation programme under grant agreement No 824140.

AUTHOR CONTRIBUTIONS

A. R. Akhmerov and P. M. Perez-Piskunow proposed the idea of hybrid KPM and initiated the project. P. M. Perez-Piskunow implemented the conventional KPM algorithms. M. Wimmer proposed and R. Skolasinski implemented the automated Löwdin perturbation theory using full diagonalization. M. Wimmer proposed using KPM for Löwdin perturbation theory, P. M. Perez-Piskunow and D. Varjas implemented hybrid Löwdin perturbation theory. S. R. Kuppuswamy applied Löwdin perturbation theory to the spin qubit example. D. Varjas and R. Skolasinski applied Löwdin perturbation theory to the nanowire example. P. M. Perez-Piskunow and M. Irfan implemented the hybrid expectation value calculation. D. Varjas proposed and implemented the hybrid expectation value perturbation theory. M. Irfan applied these methods to the Josephson junction example. A. R. Akhmerov and M. Wimmer oversaw the project and the

code development. All authors took part in writing the manuscript.

-
- [1] P. Löwdin, *A Note on the Quantum-Mechanical Perturbation Theory*, *J. Chem. Phys.* **19**, 1396–1401 (1951).
- [2] J. R. Schrieffer and P. A. Wolff, *Relation between the anderson and kondo hamiltonians*, *Phys. Rev.* **149**, 491 (1966).
- [3] J. M. Luttinger and W. Kohn, *Motion of Electrons and Holes in Perturbed Periodic Fields*, *Phys Rev* **97**, 869–883 (1955).
- [4] R. Winkler, *Spin-Orbit Coupling Effects in Two-Dimensional Electron and Hole Systems* (Springer, Berlin, Heidelberg, 2003).
- [5] Y. Saad, *Iterative Methods for Sparse Linear Systems*, 2nd ed. (Society for Industrial and Applied Mathematics, Philadelphia, PA, USA, 2003).
- [6] R. Lehoucq, D. Sorensen, and C. Yang, *Arpack users' guide: Solution of large scale eigenvalue problems with implicitly restarted arnoldi methods.*, *Software Environ. Tools* **6**, (1997).
- [7] P. R. Amestoy, I. S. Duff, J. Koster, and J.-Y. L'Excellent, *A fully asynchronous multifrontal solver using distributed dynamic scheduling*, *SIAM Journal on Matrix Analysis and Applications* **23**, 15 (2001).
- [8] P. R. Amestoy, A. Guermouche, J.-Y. L'Excellent, and S. Pralet, *Hybrid scheduling for the parallel solution of linear systems*, *Parallel Computing* **32**, 136 (2006).
- [9] A. Weiße, G. Wellein, A. Alvermann, and H. Fehske, *The kernel polynomial method*, *Reviews of Modern Physics* **78**, 275 (2006).
- [10] B. Josephson, *Possible new effects in superconductive tunnelling*, *Physics Letters* **1**, 251 (1962).
- [11] K. K. Likharev, *Superconducting weak links*, *Rev. Mod. Phys.* **51**, 101 (1979).
- [12] A. A. Golubov, M. Y. Kupriyanov, and E. Il'ichev, *The current-phase relation in Josephson junctions*, *Rev. Mod. Phys.* **76**, 411 (2004).
- [13] P. Barthelemy and L. M. K. Vandersypen, *Quantum dot systems: a versatile platform for quantum simulations*, *Annalen der Physik* **525**, (2013).
- [14] P. Yang, R. Yan, and M. Fardy, *Semiconductor nanowire: What's next?*, *Nano Letters* **10**, 1529 (2010), pMID: 20394412.
- [15] R. M. Lutchyn, J. D. Sau, and S. Das Sarma, *Majorana fermions and a topological phase transition in semiconductor-superconductor heterostructures*, *Phys. Rev. Lett.* **105**, 077001 (2010).
- [16] Y. Oreg, G. Refael, and F. von Oppen, *Helical liquids and majorana bound states in quantum wires*, *Phys. Rev. Lett.* **105**, 177002 (2010).
- [17] V. Mourik *et al.*, *Signatures of majorana fermions in hybrid superconductor-semiconductor nanowire devices*, *Science* **336**, 1003 (2012).
- [18] A. M. N. Niklasson and M. Challacombe, *Density matrix perturbation theory*, *Physical Review Letters* **92**, 193001 (2004).
- [19] C. Ishii, *Josephson Currents through Junctions with Normal Metal Barriers*, *Prog Theor Phys* **44**, 1525 (1970).
- [20] J. H. Davies, I. A. Larkin, and E. V. Sukhorukov, *Modeling the patterned two-dimensional electron gas: Electrostatics*, *Journal of Applied Physics* **77**, 4504 (1995).
- [21] C. W. Groth, M. Wimmer, A. R. Akhmerov, and X. Waintal, *Kwant: a software package for quantum transport*, *New Journal of Physics* **16**, 063065 (2014).
- [22] E. Kane, *Band structure of indium antimonide*, *Journal of Physics and Chemistry of Solids* **1**, 249 (1957).
- [23] B. A. Foreman, *Elimination of spurious solutions from eight-band $\mathbf{k} \cdot \mathbf{p}$ theory*, *Phys. Rev. B* **56**, R12748 (1997).
- [24] C. R. Pidgeon, D. L. Mitchell, and R. N. Brown, *Interband magnetoabsorption in *inas* and *insb**, *Phys. Rev.* **154**, 737 (1967).
- [25] B. Nijholt and A. R. Akhmerov, *Orbital effect of magnetic field on the majorana phase diagram*, *Phys. Rev. B* **93**, 235434 (2016).
- [26] M. Irfan *et al.*, *Hybrid kernel polynomial method*, *zenodo.3450544* (2019).
- [27] D. Varjas, T. Ö. Rosdahl, and A. R. Akhmerov, *Qsymm: Algorithmic symmetry finding and symmetric Hamiltonian generation*, *New J. Phys.* **20**, 093026 (2018).
- [28] R. J. Skolasinski, *Topology, Magnetism, and Spin-Orbit: A Band Structure Study of Semiconducting Nanodevices* (Casimir PhD Series, Delft-Leiden, 2018).

Appendix A: Chebyshev polynomial expansion of selected functions

We explicitly give the expansion of a few common functions used in condensed-matter physics and this manuscript: Delta function (used in spectral densities):

$$\delta(E - \hat{H}) = \frac{1}{\pi\sqrt{1-E^2}} \sum_m \frac{2}{1 + \delta_{m,0}} T_m(E) T_m(\hat{H}). \quad (\text{A1})$$

The Green's functions:

$$G^\pm(E, \hat{H}) = \lim_{\eta \rightarrow 0^+} \frac{1}{E - \hat{H} \pm \eta i} = \mp \frac{2i}{\sqrt{1-E^2}} \sum_m \frac{1}{1 + \delta_{m,0}} \exp(\pm i m \arccos(E)) T_m(\hat{H}). \quad (\text{A2})$$

Appendix B: Details of Löwdin expansion

We adapt this section from Ref. 28, that closely follows the derivation of arbitrary order quasi-degenerate perturbation theory in Ref. 4. The goal is to find a unitary basis transformation (Schrieffer–Wolff transformation) with skew-Hermitian matrix S ($S^\dagger = -S$) as

$$\tilde{H} = e^{-S} H e^S, \quad (\text{B1})$$

such that the transformed Hamiltonian \tilde{H} does not couple the A and B subspaces. The transformation should be the identity when the perturbation vanishes and we expand S as a series in successive orders of the perturbation

$$S = \sum_{j=1}^{\infty} \lambda^j S^{(j)}. \quad (\text{B2})$$

The transformed Hamiltonian (using the Baker-Campbell-Hausdorff formula) is

$$\tilde{H} = \sum_{j=0}^{\infty} \frac{1}{j!} [H, S]^{(j)} = \sum_{j=0}^{\infty} \frac{1}{j!} [H_0 + \lambda H'_d, S]^{(j)} + \sum_{j=0}^{\infty} \frac{1}{j!} [\lambda H'_n, S]^{(j)}, \quad (\text{B3})$$

where the nested commutator $[A, B]^{(j)}$ is defined as

$$[A, B]^{(j)} = [\dots [A, \underbrace{B, B, \dots, B}_{j \text{ times}}], \dots], \quad (\text{B4})$$

with commutator $[A, B] = AB - BA$ and we split the perturbation into block-diagonal and block off-diagonal parts as $H' = H'_d + H'_n$ with $(H'_d)_{AB} = (H'_d)_{BA} = (H'_n)_{AA} = (H'_n)_{BB} = 0$ (X_{AB} denotes the restriction of operator X to the AB block). The requirement on the S we seek is $\tilde{H}_{AB} = \tilde{H}_{BA} = 0$ and we call \tilde{H}_{AA} the effective Hamiltonian. We choose S to be block off-diagonal such that $S_{AA} = S_{BB} = 0$, this removes arbitrary unitary transformations within the A and B subspaces from the result.

To do n 'th order perturbation theory we demand the equations to be satisfied for all terms up to λ^n . Separating terms that contribute to diagonal and off-diagonal terms ($\tilde{H} = \tilde{H}_d + \tilde{H}_n$ with $(\tilde{H}_d)_{AB} = (\tilde{H}_d)_{BA} = (\tilde{H}_n)_{AA} = (\tilde{H}_n)_{BB} = 0$) we find:

$$\tilde{H}_d = \sum_{j=0}^{\infty} \frac{1}{(2j)!} [H_0 + \lambda H'_d, S]^{(2j)} + \sum_{j=0}^{\infty} \frac{1}{(2j+1)!} [\lambda H'_n, S]^{(2j+1)}, \quad (\text{B5a})$$

$$\tilde{H}_n = \sum_{j=0}^{\infty} \frac{1}{(2j+1)!} [H_0 + \lambda H'_d, S]^{(2j+1)} + \sum_{j=0}^{\infty} \frac{1}{(2j)!} [\lambda H'_n, S]^{(2j)}. \quad (\text{B5b})$$

Our goal is to recursively find $S^{(n)}$ from the lower orders $S^{(j)}$ for $j \in [1 \dots n-1]$. We solve $\tilde{H}_n = 0$ up to n 'th order by inserting the expansion $S = \sum_{j=1}^n \lambda^j S^{(j)}$ into (B5b) and letting the sums in j run to $\lfloor (n-1)/2 \rfloor$, this produces all terms up to n 'th order. We observe that at n 'th order $S^{(n)}$ only appears in a single commutator, allowing to rearrange the n 'th order terms in the equation $\tilde{H}_n = 0$ as

$$[H_0, S^{(n)}] = Y^{(n)} \quad (\text{B6})$$

where $Y^{(n)}$ only depends on lower orders of S . We generate the Y 's using symbolic computer algebra. The first few terms are:

$$[H_0, S^{(1)}] = Y^{(1)} = -H'_n, \quad (\text{B7a})$$

$$[H_0, S^{(2)}] = Y^{(2)} = -[H'_d, S^{(1)}], \quad (\text{B7b})$$

$$[H_0, S^{(3)}] = Y^{(3)} = -[H'_d, S^{(2)}] - \frac{1}{3} [[H'_n, S^{(1)}], S^{(1)}]. \quad (\text{B7c})$$

As the Y 's are purely off-diagonal Hermitian, it is possible to write only $Y_{AB}^{(n)}$ in terms of S_{AB} , S_{BA} and the restricted components of H .

The equations (B7) can be iteratively solved as

$$S_{ml}^{(j)} = \frac{Y_{ml}^{(j)}}{E_m - E_l} \quad (\text{B8})$$

where indices m and l correspond to states in the A and B subspace respectively. With the $n - 1$ order expansion of S at hand, we substitute it into (B5a) with the sum over j running to $\lfloor n/2 \rfloor$, or directly into (B3) with the sum over j running to n , to produce \tilde{H}_d up to n 'th order.

The same algorithm works in the case of multiple expansion parameters by replacing $\lambda H'$ with $\sum_{\alpha} \lambda_{\alpha} H'_{\alpha}$ and only keeping track of terms with total power j in the λ_{α} in $S^{(j)}$ and $Y^{(j)}$. Finally, we write the AA block of the transformed Hamiltonian as a sum of successive orders of the perturbation to obtain the effective Hamiltonian:

$$H_{\text{eff}} = \tilde{H}^{(0)} + \sum_{\alpha} \lambda_{\alpha} \tilde{H}^{(1,\alpha)} + \sum_{\alpha\beta} \lambda_{\alpha} \lambda_{\beta} \tilde{H}^{(2,\alpha\beta)} + \dots \quad (\text{B9})$$

Appendix C: Using KPM in higher order Löwdin expansion

To use KPM efficiently, we want to avoid using an explicit basis for the B subspace. We observe that the expressions (B7) for Y and (B5a) for \tilde{H}_{AA} can be expanded in terms of the restricted operators (i.e. H'_{AA} , H'_{AB} , etc.). Whenever two terms with A indices are adjacent, we may insert a projector onto the A states $P_A = \sum_m |m\rangle\langle m|$ with a full basis of A states $|m\rangle$. Whenever two terms with B indices are adjacent, we insert a projector onto the B subspace $P_B = \mathbb{1} - \sum_m |m\rangle\langle m|$. This allows to remove the restriction from one of the adjacent terms, for example

$$\langle m|S_{AB}H'_{BB}S_{BA}|m'\rangle = \langle m|P_A S P_B P_B H' P_B P_B S P_A|m'\rangle = \langle m|S H' S|m'\rangle = \sum_{ij} S_{mi} H'_{ij} S_{jm'} \quad (\text{C1})$$

where we used that S is only nonzero in the off-diagonal blocks. This allows to only store the mixed matrix elements $S_{mi} = \langle m|S|i\rangle$ where $|i\rangle$ is the original basis where the Hamiltonian is sparse with indices i, j running over the full Hilbert space, and $|m\rangle$ is the basis of the A subspace. In this basis $\sum_i S_{mi} (P_B)_{ij} = S_{mj}$, similarly for block off-diagonal matrices. It is possible to replace all H_{BB} terms with H because there is only one H in every product, all the other terms are S 's. This is advantageous as H' acting on the full Hilbert space of size N can be represented as a sparse matrix of $\mathcal{O}(N)$ nonzero entries, while S_{mi} and other off-diagonal components can be stored as small dense matrices with $\mathcal{O}(Na)$ entries where $a = \dim(A)$.

Now we rewrite (B8) in terms of the Green's function:

$$S_{mi}^{(n)} = \sum_j Y_{mj}^{(n)} \left(\frac{1}{E_m - H_0} \right)_{ji} = \sum_j \left[G_0(E_m)_{ij} \left(Y^{(n)\dagger} \right)_{jm} \right]^{\dagger} \quad (\text{C2})$$

where we used that Y is block off-diagonal and $G_0(E)$ does not mix the A and B subspaces. For numerical stability reasons, we still apply P_B from the right in practice. Following the procedure outlined in Appendix B we successively generate all S terms and produce \tilde{H}_{AA} , the only difference is using the above basis convention.

The computational complexity of generating the n 'th order effective Hamiltonian (in the case of a single small parameter) is $\mathcal{O}(n^2 a N M)$, where M is the number of KPM moments, practically chosen to be at the order of bandwidth/gap. We obtain this estimate by the following reasoning: A single evaluation of the KPM Green's function on a vector costs $\mathcal{O}(NM)$. To get $S^{(j)}$, we need to apply G to (aj) vectors on the right hand side, as $Y^{(j)}$ is a j 'th order polynomial of the small parameter. We argue that the KPM step is the costliest part of the procedure, because evaluation of Y and \tilde{H} only involves products of small or sparse matrices.

There is, however, a combinatorial factor in the number of terms involved in these expressions, which grows exponentially with j . At high orders $Y^{(n)}$ contains $\mathcal{O}(2^n)$ terms with a single small parameter. At high enough orders, it is more efficient to directly evaluate the commutator series giving $Y^{(n)}$ by substituting the $n - 1$ order expansion of S with numerical coefficients. Truncating to terms of at most order n after every multiplication, this only takes $\mathcal{O}(n^3)$ time. Hence, this latter method becomes more efficient for high enough orders. Combinatorial factors are even larger if there are multiple small parameters in the expansion. We defer further analysis of the complexity and possible optimizations of high order expansions.